

CON-SST-RAIN

Continuous Stochastic Space–Time Rainfall generation based on Markov chains and transposition of weather radar data

Andersen, Christoffer B.; Wright, Daniel B.; Thorndahl, Søren

Published in:
Journal of Hydrology

DOI (link to publication from Publisher):
[10.1016/j.jhydrol.2024.131385](https://doi.org/10.1016/j.jhydrol.2024.131385)

Creative Commons License
CC BY 4.0

Publication date:
2024

Document Version
Publisher's PDF, also known as Version of record

[Link to publication from Aalborg University](#)

Citation for published version (APA):
Andersen, C. B., Wright, D. B., & Thorndahl, S. (2024). CON-SST-RAIN: Continuous Stochastic Space–Time Rainfall generation based on Markov chains and transposition of weather radar data. *Journal of Hydrology*, 637, Article 131385. <https://doi.org/10.1016/j.jhydrol.2024.131385>

General rights

Copyright and moral rights for the publications made accessible in the public portal are retained by the authors and/or other copyright owners and it is a condition of accessing publications that users recognise and abide by the legal requirements associated with these rights.

- Users may download and print one copy of any publication from the public portal for the purpose of private study or research.
- You may not further distribute the material or use it for any profit-making activity or commercial gain
- You may freely distribute the URL identifying the publication in the public portal -

Take down policy

If you believe that this document breaches copyright please contact us at vbn@aub.aau.dk providing details, and we will remove access to the work immediately and investigate your claim.



Research papers

CON-SST-RAIN: Continuous Stochastic Space–Time Rainfall generation based on Markov chains and transposition of weather radar data

Christoffer B. Andersen^{a,b,*}, Daniel B. Wright^b, Søren Thorndahl^a

^a Aalborg University, Department of the Built Environment, Aalborg, Denmark

^b University of Wisconsin-Madison, Department of Civil and Environmental Engineering, WI, USA

ARTICLE INFO

This manuscript was handled by Andras Barossy, Editor-in-Chief, with the assistance of Felix Frances, Associate Editor.

Keywords:

Spatio-temporal rainfall
Markov Chains
Stochastic rainfall generation
Weather radar data
Stochastic storm transposition

ABSTRACT

In this study, we present CON-SST-RAIN, a novel stochastic space–time rainfall generator specialized for model-based urban drainage design and planning. CON-SST-RAIN is based on Markov Chains for sequences of dry/rainy days and uses stochastic storm transposition (SST) to generate realistic rainfall fields from weather radar data. CON-SST-RAIN generates continuous areal rainfall time series at arbitrary lengths. We propose a method for updating the Markov Chains by each passing year to better incorporate low-frequency variation in inter-annual rainfall values. The performance of CON-SST-RAIN is tested against multi-year records from rain gauges at both point and catchment scales. We find that updating the Markov Chains has a significant impact on the inter-annual variation of rainfall, but has little effect on mean annual/seasonal precipitation and dry/wet spell lengths. CON-SST-RAIN shows good preservation of extreme rain rates (including sub-hourly values) compared to observed rain gauge data and the original SST framework.

1. Introduction

Rainfall time series is a crucial aspect in design and planning of hydrological structures and water infrastructure. Historical time series used for model-based design purposes can be lacking temporal information (gaps in time or insufficient periods of observation to estimate relevant return levels), or spatial information (e.g. point rainfall with inadequate spatial representation of rainfall fields) (Cristiano et al., 2017; Ochoa-Rodriguez et al., 2015). Traditionally, historical long time series of point rainfall are used for assessing point rainfall statistics to create design storms (Madsen et al., 2017; Gregersen et al., 2013) or applied directly in hydrological model simulations to estimate return levels of hydrological system response (Thorndahl, 2009). The application of point rainfall works well if the hydrological catchment in question is small, and the impact of spatial rainfall variability is insignificant. However, if a catchment is subject to uneven hydrological loading due to the movement and dynamics of rainfall, the spatial component cannot be neglected without compromising the accuracy of the estimated system response (Ochoa-Rodriguez et al., 2015; Tuyls et al., 2018; Cristiano et al., 2019). If applied directly in hydrological modelling, dense rain gauge networks or weather radar observations that have a representation of the spatial variability might resolve these challenges, but these are rarely available over sufficient periods and with consistent data quality to estimate return levels of e.g. 10 or more years. To support, or even circumvent, these issues several

stochastic rainfall generators have been developed to model key aspects of rainfall fields and thus enable filling of missing information in time or space or to generate arbitrary long chains of continuous rainfall that exceed the length of observed records (Wilks and Wilby, 1999; Sharma and Mehrotra, 2010). These types of rainfall models only serve to simulate statistical properties of rainfall and rainfall fields and are therefore not chronologically comparable to rainfall observations nor to numerical weather or climate models. Unlike observational data, the rainfall generators do have the possibility to be customized for specific hydrological applications and with length and space–time resolution to resolve the challenges of the case in question.

In the literature, rainfall generators are often categorized as either: parametric (Brissette et al., 2007) or non-parametric (Rajagopalan and Lall, 1999). Parametric models involve choosing distribution functions to model both spatio-temporal occurrences (e.g. Markov Chains for sequences of dry and rainy days) of rainfall (both at single and multi-site models) and precipitation amounts (e.g. exponential model of daily rainfall amounts). Some parametric models generate exclusively synthetic rainfall space–time series based on stochastic-statistical processes and therefore have to be evaluated against observations (e.g. Fowler et al., 2005 and Burton et al., 2008). Other types of parametric rainfall generators combine physical dynamics of climatological variables with stochastic realizations to generate spatiotemporal rainfall fields

* Corresponding author at: Aalborg University, Department of the Built Environment, Aalborg, Denmark.
E-mail address: cband@build.aau.dk (C.B. Andersen).

(e.g. Peleg et al., 2017). Non-parametric models attempt to avoid the subjective decision of a statistical distributions by instead resample a given time series stochastically.

As stated earlier a rainfall generator is a supportive tool in the field of hydrology and can thus have a broad field of application. Thorndahl et al. (2017a) and Thorndahl and Andersen (2021) developed a single-site hybrid generator (CLIMACS) that resamples observed rain gauge observation at event scale. CLIMACS can recreate the same statistical metrics (annual and seasonal precipitation, number of extreme days, and drought periods) as observed historically. It is furthermore used to downscale regional climate models to create rainfall time series representative for future climate scenarios for application in urban drainage models. Multi-site generators, such as the mulGETS model (Brissette et al., 2007), have been developed for impact studies of daily rainfall. Zhou et al. (2019) expanded on the idea of multi-site generation and handled a common weakness/criticism of rainfall generator's inability of retaining low-frequency variation (Sharma and Mehrotra, 2010). More recently Peleg et al. (2017) presented a methodology to produce sub-daily and gridded rainfall/weather products for climatological uncertainty analysis (Peleg et al., 2019). Each of the mentioned rainfall generators are developed with a specific interest in mind. This study aims to investigate how to develop a framework that is suitable for hydrological modelling of dense urban areas thus outputting high-resolution rainfall products.

Rainfall input for urban hydrological design and planning has been shown to require high resolution in both the temporal and spatial domain (Einfalt et al., 2004; Thorndahl et al., 2017b). The advancement in weather radar observation technology over the past decades has increased temporal and spatial resolution of radar data. The recency of the technology, however, hinders long-term statistical assessment due to short time series compared to traditional rain gauge time series. Furthermore, radar rainfall data quality can be challenged by attenuation, clutter, bias-adjustment, etc. which leads to rejection or filtering of data in space or time and complicates direct hydrological applications (Thorndahl et al., 2017b; Einfalt et al., 2004; Villarini and Krajewski, 2010; Nielsen et al., 2024).

Stochastic Storm Transposition (SST) is a technique that involves resampling of observed rainfall, in both time and space, to generate a hypothetical yet realistic representation of rainfall events (Wright et al., 2020). Wright et al. (2013) presented a framework, for the SST method, where rain events, at user-specified durations are aggregated in a storm catalog. These events are randomly selected and transposed to virtually extend observation periods for the applied radar data and thus enabling more detailed frequency analysis. It has been applied for flood frequency analysis in Wright et al. (2014) and utilized as an exploratory tool in Zhou et al. (2021) to investigate runoff sensitivity in an urban watershed. The framework is further explored in Andersen et al. (2022) in a different climatology than in the previously mentioned studies and with a different radar dataset that also includes sub-hourly rainfall estimates. The SST framework shows great promise in recreating extreme rainfall statistics similar to other ground-based measurements with significantly longer periods of observation.

In the present study we introduce the novel framework CON-SST-RAIN (phonetically: constrain) to combine radar data into a Continuous Stochastic Space-Time RAIN series specialized for urban applications, by a hybrid approach of using Markov Chains for wet/dry sequence modelling and time/space resampling of observed radar rainfall, similar to the SST framework. Current weather radars offers extremely high resolution in the spatio-temporal domain (down to 100×100 meter at 1 min (Ochoa-Rodriguez et al., 2015; Nielsen et al., 2014; Schleiss et al., 2020)) which is a desirable trait in the planning and design of urban drainage systems. This high resolution is however often severely limited either by observation period or data availability and therefore not directly applicable as input for long-term hydrological modelling. Consequently, CON-SST-RAIN aims towards virtually stitching together a section of observed (matching a specified urban catchment) radar

rainfall into an arbitrary long continuous series. We investigate how well CON-SST-RAIN maintains crucial statistical features: mean annual and seasonal precipitation, year-to-year variation of seasonal precipitation (low-frequent variability), extreme rain rates, and spatial correlation at multiple rainfall sites. CON-SST-RAIN is also able to produce ensembles of multi-year records of areal rainfall allowing for the inherent uncertainty to be investigated. We test different types of Markov Chains and how they affect the aforementioned statistical metrics and we suggest an approach to update Markov Chains for each simulated year to better represent the low-frequency variation of rainfall values.

The paper is structured as follows: A presentation of applied data sets is given in Section 2. Section 3 presents all the applied methods: Overall structure of CON-SST-RAIN (Section 3.1), Markov Chains (Section 3.2), SST methodology 3.3, and evaluation metrics of CON-SST-RAIN (Section 3.4). Section 4 presents and discusses CON-SST-RAIN's ability to generate continuous space-time series and recreate rainfall statistics. Concluding remarks are made in Section 5.

2. Data

2.1. Study area

We identify the Island of Zealand, Denmark as our primary study domain (Fig. 1). We focus specifically on generating areal rainfall time series for the greater Copenhagen area (red area in Fig. 1). The domain covers approx. 8000 km² and is covered well by rain gauge stations and radar data as described in the following sections. The greater Copenhagen area (approx. 150 km²) is densely populated and consists of urban and sub-urban areas in which stormwater is discharged through both combined and separate sewer systems.

2.2. Rainfall data

2.2.1. Rain gauge data

The collection of rain gauges scattered around the study area (Fig. 1), is part of a larger network of rain gauges managed by the Water Pollution Committee in Denmark (WPC, 2007). All of the rain gauges are of the tipping-bucket type and record rainfall with a bucket size of 0.2 mm. The registrations are processed into time series with a 1-minute resolution. For post-processing in this particular study the gauge rainfall series are aggregated to 10 min resolution to match the radar rainfall dataset. All of the recorded rainfall intensities are grouped into singular events. An event is defined by the triggering of the first tip of a bucket and ended with 60 consecutive minutes with no tips. If only one tip is registered the event is discarded.

We utilize the rain gauge data series as our ground truth in the validation of CON-SST-RAIN. The dataset is split into two subsets: long-term data and short-term data. The long-term data consists of gauges with the longest common period of observation (1979–2021, 42 full years) and will be used for validating temporal-dependent variables (i.e. mean annual precipitation and low-frequent variability). The short-term gauges (note that data from the long-term dataset is also included here) present a decent spatial representation of rainfall over the area of interest and allow us to investigate CON-SST-RAIN's ability to create spatial structures as observed by the rain gauge network.

2.2.2. Weather radar data

The applied radar dataset originates from a single C-band radar, located approximately 50 km south of the area of interest (Fig. 1). The radar is managed and operated by the Danish Meteorological Institute (DMI) and has been in operation since 2002.

The complete processing of the radar-rainfall data has been detailed in Thorndahl et al. (2014a) and a brief resumé of the process chain will be presented in the following.

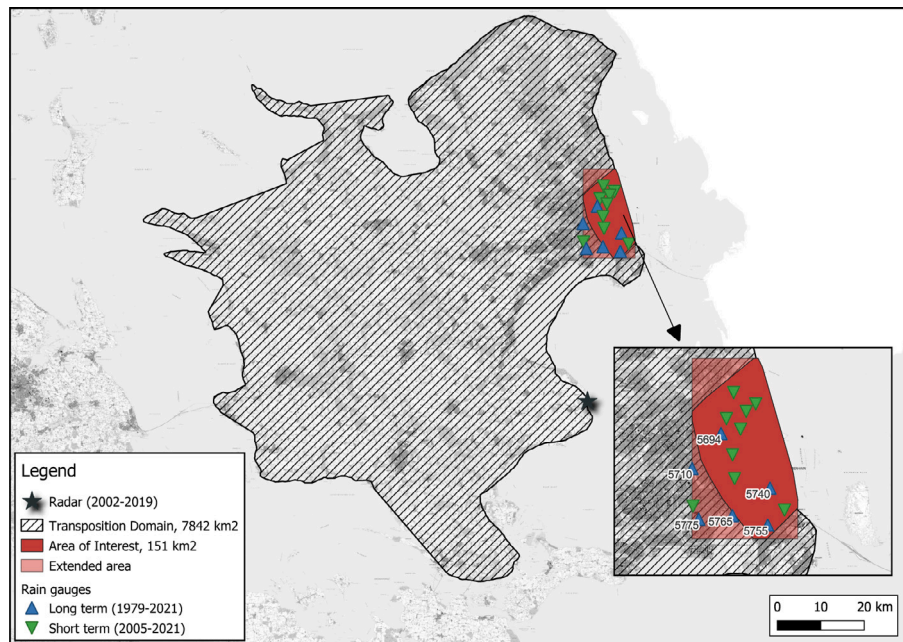


Fig. 1. Overall study area and area of interest (red) for areal rainfall generation. Shaded area denotes the transposition domain that relates to the SST framework Section 3.3. The two sets of rain gauge data: Long-term and short-term rain gauge sites and the radar (star) are shown and the observation period denoted. (For interpretation of the references to colour in this figure legend, the reader is referred to the web version of this article.)

Table 1

Mean field bias, Root mean square error (RMSE) and Mean absolute error (MAE) for rainfall durations ranging from 10 min to 24 h.

Rainfall duration [min]	10	30	60	180	360	720	1440
Bias [-]	1.56	1.27	1.19	1.11	1.06	1.03	1.00
RMSE [mm/h]	8.71	4.43	3.09	1.42	0.83	0.47	0.25
MAE [mm/h]	4.49	2.28	1.46	0.69	0.41	0.23	0.12

For this study, a reflectivity product, from 2002 to 2019, is generated. The scanings are made at a pseudo constant altitude of 1 km, 10-minute resolution, and processed from a polar grid with an azimuth resolution of 1° to Cartesian grid with a $500 \text{ m} \times 500 \text{ m}$ resolution. The reflectivity is transformed into rain rates by applying a standard Marshall-Palmer Z-R relationship ($A=200$, $B=1.8$). A daily mean-field bias approach (Smith and Krajewski, 1991; Thorndahl et al., 2014b), utilizing up to 100 rain gauges (not shown in this study) within the radar domain (Fig. 1), is applied to derive valid quantitative precipitation estimates.

The original 10-minute temporal resolution based on single snapshots is downscaled to a 1-minute resolution by advective interpolation as presented in Nielsen et al. (2014). This has been shown to further improve the quantitative precipitation estimates of the radar-rainfall product when applied prior to the mean-field bias adjustment (Thorndahl et al., 2014a). In this study, we choose to convert the radar-rainfall back to a 10-minute resolution for computational purposes and thereby maintain the improved rainfall estimates that derive from the advection interpolation.

Table 1 shows duration-specific biases after the radar dataset has been daily mean-field bias adjusted. As detailed in Thomassen et al. (2022), Schleiss et al. (2020), Thorndahl et al. (2019), Andersen et al. (2022) there is a tendency, for rainfall intensities as a function of shorter rainfall durations, to be underestimated by the radar in comparison to rain gauge data. The reason for this is primarily a spatial scaling issue which is constituted by the difference between point and pixel as an artifact of the implemented daily mean-field bias adjustment of radar data against rain gauges (Thorndahl et al., 2014a).

The radar dataset is applied and tested in other studies, e.g. in extreme value statistics (Schleiss et al., 2020; Andersen et al., 2022)

and in spatial correlation studies (Thomassen et al., 2022; Thorndahl et al., 2019).

Defining single independent rain events is challenging for spatially distributed rainfall unlike for point rain gauge data as described earlier. We, therefore, choose to group the radar-rainfall dataset into full-day observations running from midnight to midnight (00 UTC). These diurnal datasets will consist of both dry and wet periods. A total of 1104 rainfall days over the period of 17 full years is included in the study. The rainfall days are selected by a threshold of a minimum 3 mm of rain in at least one rain gauge within the radar domain to ensure a valid bias adjustment. Furthermore, some days are discarded due to clutter, noise, or poor bias adjustment, leaving the dataset abrupt in time. A drizzle threshold of 0.1 mm/hr is implemented based on the premise in Thomassen et al. (2022). Rain intensities below this threshold are thus considered as no rain. This helps to distinguish single events and improves the assessment of the binary distribution between dry and wet periods in the dataset.

2.2.3. Regional extreme rain rate model

Besides statistics derived directly from the rain gauges presented in Fig. 1 we utilize a regional partial duration series (PDS) model (formally known as the Danish regional rainfall model of the Danish Water pollution Committee, hereafter referred to as the WPC model). This model is based on a large collection of rain gauges (83 gauges with a total of 1881 station years) (Madsen et al., 2017). The gauges utilized in this study are likewise part of the regional model. The output of the WPC model is extreme value rain rates for specified rainfall durations (ranging from 1 min to 48 h) and user-specified return levels. The model's conceptualization and development are detailed in Madsen et al. (2017) and Gregersen et al. (2013) and shortly presented here. A Generalized Pareto Distribution is fitted to rain intensities above a threshold value for multiple durations. The regional variability is implemented by correlating the Pareto distribution function parameters to different climatological dependent variables (e.g. mean annual precipitation or the maximum daily rainfall depth). This allows for regional differences in extreme rainfall intensities to be modelled consistently and reduces the effect any potential outliers may have on the final extreme value analysis (Madsen et al., 2017).

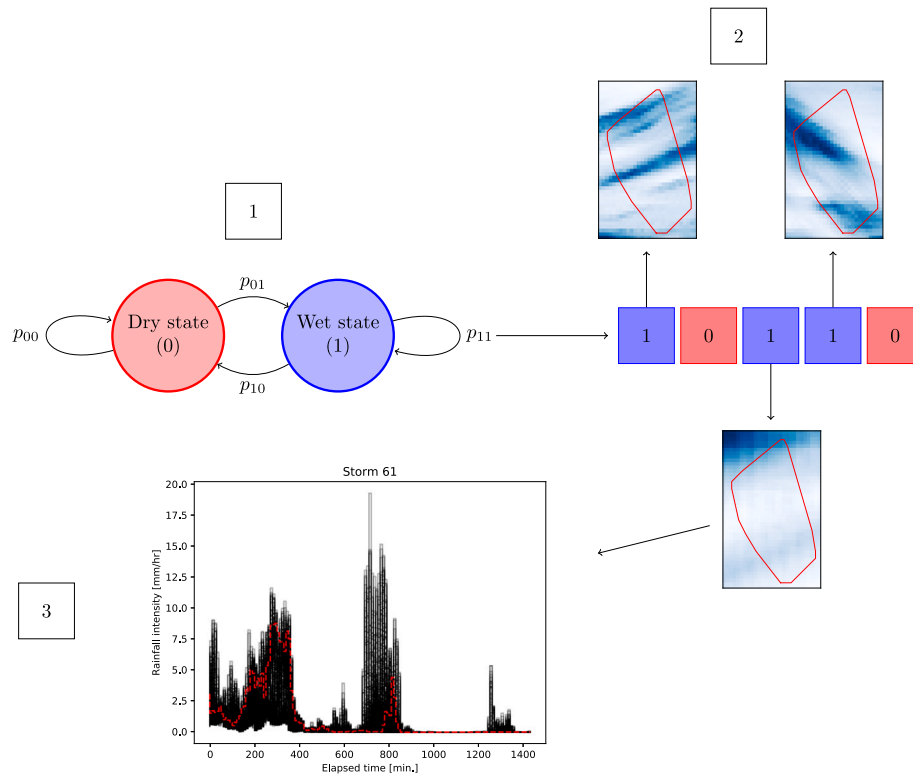


Fig. 2. Schematic diagram of CON-SST-RAIN. (1) A Markov Chain that governs the day-to-day state of whether rainfall should occur over the specified area of interest or not. (2) Rain events (storms) are stochastically transposed over the area of interest (marked by red contouring line), (3) Spatio-temporal dynamics of the rainfall field are retained (black lines indicate individual pixel values, red line pixel with largest rainfall depth over the duration of the storm). (For interpretation of the references to colour in this figure legend, the reader is referred to the web version of this article.)

3. Methods

3.1. Stochastic time-area rainfall generation by CON-SST-RAIN

CON-SST-RAIN combines a traditional approach of simulating sequences of days with and without rain using Markov Chains and Stochastic Storm Transposition to resample observed rainfall in the spatio-temporal domain. The overall structure of CON-SST-RAIN is presented in Fig. 2.

The Markov Chain simulates day-to-day states of either rainfall or no rainfall. The Markov Chain is directly derived from the long-term rain gauges highlighted in Fig. 1. This process is further detailed in Section 3.2.

For each simulated day with rainfall (wet-state) a random day is sampled from the catalogue of daily storms and stochastically transposed in space, in order to be substituted into the generated continuous space-time series. This part is a modification of the SST framework (Wright et al., 2017) with some additions as detailed in Section 3.3.

Due to the inherent variance from both the Markov Chains and the SST framework we use CON-SST-RAIN to simulate an ensemble of 100 realizations of multi-year areal rainfall. The evaluation of CON-SST-RAIN is detailed in Section 3.4.

3.2. Sequence modelling of rainfall days

A Markov Chain is a stochastic model that simulates a sequence of outcomes from a predefined state space. A simple first order Markov Chain can be described by the two conditional probabilities (1) and (2) (visual representation in Fig. 2).

$$p_{00} = P(\text{dry day} \mid \text{prior day is dry}) \quad (1)$$

$$p_{01} = P(\text{wet day} \mid \text{prior day is dry}) \quad (2)$$

Markov Chains are a basis for many stochastic rainfall generators (Wilks and Wilby, 1999; Brissette et al., 2007; Sharma and Mehrotra, 2010; Zhou et al., 2019). The examples above (Eqs. (1) and (2)) of a Markov Chain show its very basic level. The concept can further be expanded upon either by increasing the order, i.e. second-order Markov Chain where the state of the present day is conditioned on the states of the two prior days (i.e. the probability that it will rain today given the two prior days are dry).

Seasonality of rainfall occurrence can also be simulated by using non homogeneous Markov Chains (NHMC) (Sharma and Mehrotra, 2010), by removing the stationarity of the chain and allowing it to change over time (i.e. the chain used in winter season is different from the one used in spring season, as presented in Fig. 3).

The transition probabilities for this study is derived directly from the rain gauge data set presented in Section 2.2. The entire observed rain gauge time series is aggregated to a time series of daily rainfall. A day is considered to be in the dry state if the accumulated rain depth is less than 0.2 mm and wet otherwise. The 0.2 mm matches the resolution of the tipping gauge bucket and is similar to other studies of stochastic rainfall generators (Brissette et al., 2007; Zhou et al., 2019).

A general flaw, and common criticism, of Markov Chains, is that they end up as year-long averages of rainfall occurrences, which can lead to underestimation of natural low frequent variability (year-to-year variation of critical values such as mean annual and seasonal precipitation) (Sharma and Mehrotra, 2010). To avoid this we suggest to stochastically update the Markov Chains from year to year in order to allow greater inter-annual variability. Using the aforementioned approach of deriving the transition probabilities for the Markov Chains, we derive separate Markov Chains for each of the observed years

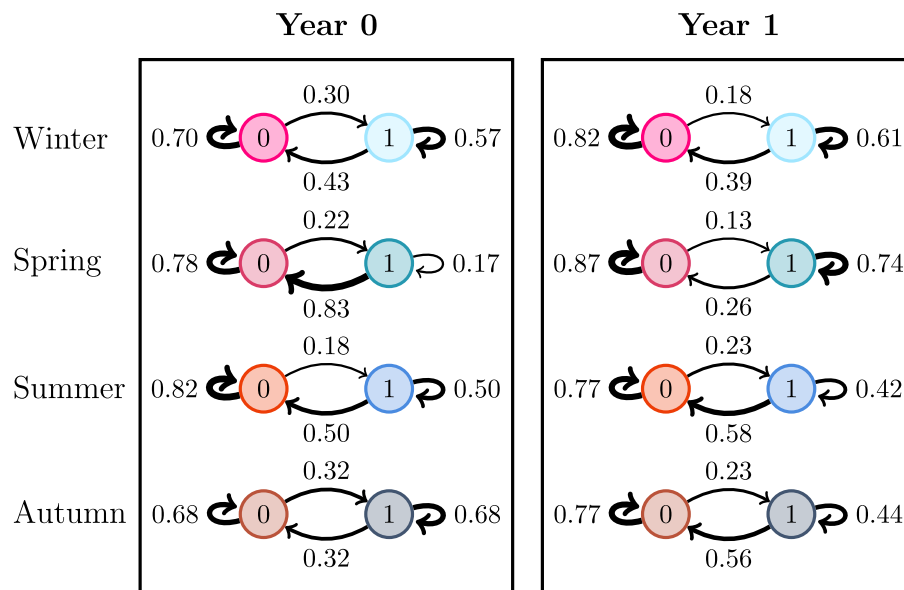


Fig. 3. Representation of a first-order, two-state, non-homogeneous Markov Chain (NHMC) that is updated stochastically for each passing year. The states 0/1 represent dry/wet conditions respectively. Transition probabilities are noted above each arrow and the thickness of the arrows is proportional to the transition probability.

and pool them. When simulating sequences of dry and wet days a Markov Chain is randomly chosen from the pool of historically derived chains for each simulated year. This concept is presented in Fig. 3. We choose to investigate a first- and second-order non-homogeneous Markov Chain using the traditional method applying one chain for all simulated years (in the following referred to as configurations: (a) 1st order NHMC and (b) 2nd order NHMC), as well as the proposed method of choosing stochastically updated chains for all simulated years (in the following referred to as configurations: (c) 1st order updated NHMC and (d) 2nd order updated NHMC).

We assume that the applied Markov Chain is valid for the entire area of interest (Fig. 1). As a consequence we are not able to distinguish between days with rain only at parts of the area of interest and total rain cover, as would be the case with multi-site Markov Chains such as the mulGETS model presented in Brissette et al. (2007). This assumption is necessary because of the natural spatial randomness of rainfall in the sampled days which follows the stochastic spatio-temporal resampling of the SST framework.

3.3. Stochastic Storm Transposition

Stochastic Storm Transposition (SST) is a probabilistic framework where synthetic yet realistic rainfall statistics are generated by sampling and spatially shifting (transposing) observed rain storms (Wright et al., 2020). The framework can virtually extend the data set, allowing for high detail frequency analysis (Wright et al., 2013), and when coupled with hydrological models, flood frequency analysis (Wright et al., 2014; Zhou et al., 2021).

The core concept of the SST framework is selecting a spatial extent, henceforth known as transposition domain, in which the climatology is considered/assumed to be homogeneous. In this domain, a rainfall event will have an equal probability of occurring anywhere within the domain, thus enabling one to transpose the rainfall stochastically in the x - y direction. The transposition domain for this study can be seen in Fig. 1 and is assumed to be climatologically homogeneous according to the findings in Andersen et al. (2022).

Wright et al. (2013) formulates a methodology in which radar rainfall is catalogued by storm duration into storm catalogues and is coupled with an annual storm occurrence model (Poisson Distribution), allowing one to create a specified number of years of extreme rainfall for extreme value statistics. Here, we adopt parts of this methodology,

Table 2

Seasonal distribution of the number of wet days in the radar catalogue and correspondingly rain gauge with more than 3 mm rainfall in station no. 5694, from 2002 to 2019. Numbers in parentheses indicate relative occurrence.

Season	Winter	Spring	Summer	Autumn
Radar catalogs	178(0.16)	199(0.18)	421(0.38)	306(0.27)
Gauge ≥ 3 mm	256(0.23)	215(0.19)	337(0.31)	297(0.27)

namely the storm catalogue generation, but we limit the extent to a single storm duration. The radar dataset, presented in Section 2.2, is thus catalogued into 24-hour catalogues and posteriorly separated into seasons to match the NHMC presented in Section 3.2. For each day noted to contain rain from the NHMC, we select, at random, a season appropriate storm from the 24-hour radar catalogue ((2) on Fig. 2). This leads to another assumption that storms on this time scale can be sampled independently. Similar assumption was made for the CLIMACS model (Thorndahl et al., 2017a) and evidence of this independence has been shown in Thomassen et al. (2022). The distribution of the number of storms per season is listed in Table 2 for the radar data storm catalogue and the rain gauge data, respectively.

The winter season in the radar catalogue contains fewer wet days compared to the gauge dataset, which could be a result of the more stringent filtering of radar data during this season. This could be caused by issues such as poor bias adjustment or an increase in noisy data caused by solid precipitation. On the other hand, the radar dataset records a higher number of rainy days in the summer season. This discrepancy may be attributed to the comparison of spatial rainfall data with a point-based rain gauge dataset. Summer months tend to be more susceptible to localized convective storms with limited spatial coverage. These storms may not be captured by a single rain gauge station, but would be included in the radar dataset.

The methodology presented in Wright et al. (2013) has later been compiled into the OpenSource python tool “RainyDay” (Wright et al., 2017). We utilize RainyDay to estimate IDF curves for storm durations ranging from 10 min to 24 h. We use the same approach and modifications as detailed in Andersen et al. (2022); where the top 500 storms, according to the shape and size of the area of interest, are selected for frequency analysis. The annual storm occurrence is fixed at 88 storms per year.

3.4. Evaluation metrics

To evaluate and compare the four different configurations of the Markov Chains and to evaluate the CON-SST-RAIN's ability to recreate statistics similar to statistics of observed time series, we divide the evaluation into two parts. First, we determine the statistical metrics that characterize the temporal patterns of rainfall, and second, we develop statistical metrics that reflect the spatial coherence.

The following statistical metrics are employed to characterize temporal variability at point scale:

- Wet and dry spell lengths on a daily scale.
- Mean annual and seasonal precipitation.
- Low-frequency variability (year-to-year variation of seasonal and monthly precipitation) calculated by the variance between the different realizations.
- Extreme value statistics at rainfall durations ranging from 10 min to 24 h and with return levels of 1 year to 10 years.

Wet and dry spell lengths are considered as the number of consecutive days with either rain or no rain. Whether a day is considered wet or dry follows the same procedure of the derivation of transition probability distributions in the Markov Chain procedure (see Section 3.2).

Extreme value statistics are represented as Intensity-Duration-Frequency (IDF) curves for rainfall durations: 10, 60, 30, 180, 360, 720, and 1440 min and return levels of 1, 2, 5, and 10 years. The frequency analysis is performed as a general Peaks-Over-Threshold approach. We follow the recommendations from Gregersen et al. (2013) and choose our threshold value to observe three exceedances annually on average. The return levels are estimated using California plotting position ranking (3).

$$T = \frac{N}{r} \quad (3)$$

Where T denotes the return level, N is the total number of observation years, and r is the rank of sorted rainfall intensities (in descending order). While a median plotting position or Gringorten formula (Gringorten, 1963) would be statistically more appropriate to empirically estimate return periods; the other datasets utilized in this study is based on the California plotting position, thus maintaining comparability.

We also use the RainyDay software package (Wright et al., 2017), with similar modifications as detailed in Andersen et al. (2022), to derive IDF curves using the applied radar dataset for the same durations and return levels.

The temporally dependent metrics are examined at point scale. The climatology for the study area can be assumed reasonably homogeneous (Andersen et al., 2022). Consequently, the homogeneity assumptions imply that the statistics will vary insignificantly on average at the catchment scale. The statistical metrics is derived from the long-term gauges presented in Fig. 1 and covers the period of 6-01-1979 to 31-12-2020 (about 42 years in total). These metrics are compared to a total of 100 realizations generated by CON-SST-RAIN covering the same period.

The Following statistical metrics regarding spatial coherence are investigated:

- Spatial correlation of daily rainfall.
- IDF curves at catchment scale.

Based on the short-term gauges (Fig. 1), we derive spatial correlation functions at the daily time scale and compare them to correlation functions estimated based on the individual pixels from the 100 realizations of CON-SST-RAIN. Pairwise correlation of daily rainfall is calculated by Pearson's coefficient of correlation, p , (4) and is fitted

to a two-parameter exponential expression as a function of distance, d , (5):

$$p_{i,j} = \frac{cov(R_i, R_j)}{\sqrt{var(R_i) var(R_j)}} \quad (4)$$

$$p(d) = \exp\left(-\frac{d^\alpha}{\beta}\right) \quad (5)$$

R_i and R_j corresponds to daily rainfall time series for a gauge/pixel pair (i and j , respectively). α and β are coefficients used in the exponential fit. Müller-Thomy et al. (2018) shows that an intensity dependent relation for the Pearson's coefficient of correlation exists and thus distinguishes between days above 4 mm and days below. We adopt this approach however, slightly modified by choosing 3 mm as our threshold to match the threshold used in selection of radar data. We calculate correlation functions for two scenarios: continuous series (one of the pairs can be zero) and simultaneous ($R_i > 0$ and $R_j > 0$).

The rainfall generated by CON-SST-RAIN is converted to a catchment-average time series from which we derive IDF curves using the same approach as for the point scale IDF curves. Finally, we compare these IDF's to those obtained using the RainyDay method, similar to the point scale, however, sampling from the area of interest.

4. Results

We generate in total 400 different realizations of CON-SST-RAIN, 100 for each of the different Markov Chain configurations detailed in 3.2. Fig. 4 shows examples of point time series from CON-SST-RAIN and an observed time series as reference (top panel). The exemplified series are four random selections from the pool of realizations based on the updated second-order Markov chain.

Scale issues becomes clear on Fig. 4 by all peaks produced by CON-SST-RAIN (bottom four panels) being underestimated relative to the observed timeseries (top panel). This is further investigated in Section 4.4.

4.1. Wet and dry spell lengths

An advantage of using stochastic rainfall generators over traditional design storms is the possibility of retaining rainfall's temporal continuity. The sequencing of both wet and dry days can be crucial for hysteretic hydrological systems, e.g., systems depending on antecedent soil moisture conditions or systems with detention storage (Nielsen et al., 2019). Therefore, a continuous rainfall generator should be able to adequately recreate wet and dry spells. Fig. 5 shows a QQ-plot of observed (gauge 5755 from Fig. 1) and simulated (ensemble of 100 realizations of the pixel with the exact location as gauge 5755) wet/dry spell lengths, for a 42 year period. The subplots (a-d) refer to the different configurations of the Markov Chains.

All of the configurations of types of Markov chains show a general agreement with the observed rain gauge data. Generally, all the Markov chains fail in recreating drought periods of 60+ day; only parts of the second-order stochastically updated chain model ensemble can do so. A model developed by DMI (Thejll et al., 2022) for climate projection of rainfall simulates the longest dry spell length at around 26 days (for the period of 1981–2010), suggesting that the 60+ dry spell days either is an extreme case or caused by measurement error/malfunctions/downtime in the gauge data. If, for this reason, the 60-day quantile is discarded from the dataset, the general agreement between gauge data and the Markov chains is more or less equal. The stochastically updated Markov chains (column c and d in Fig. 5) appears to perform slightly better, specifically for dry spell lengths, in the upper percentile (except for the 60 days quantile), most likely because the updating allows for more extreme drought seasons to occur.

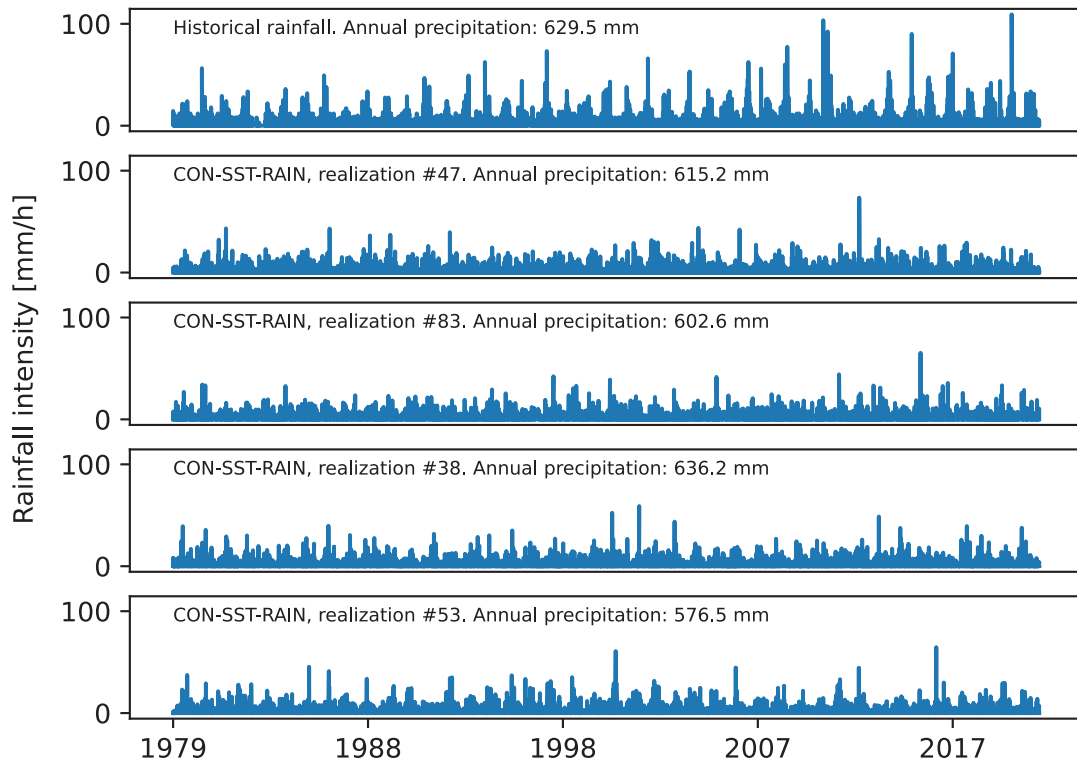


Fig. 4. Time series for rainfall intensity for gauge 5694 (top row) and four, random, CON-SST-RAIN realizations (for a single pixel corresponding to the location of gauge 5694). The temporal resolution of the timeseries is 10 min.

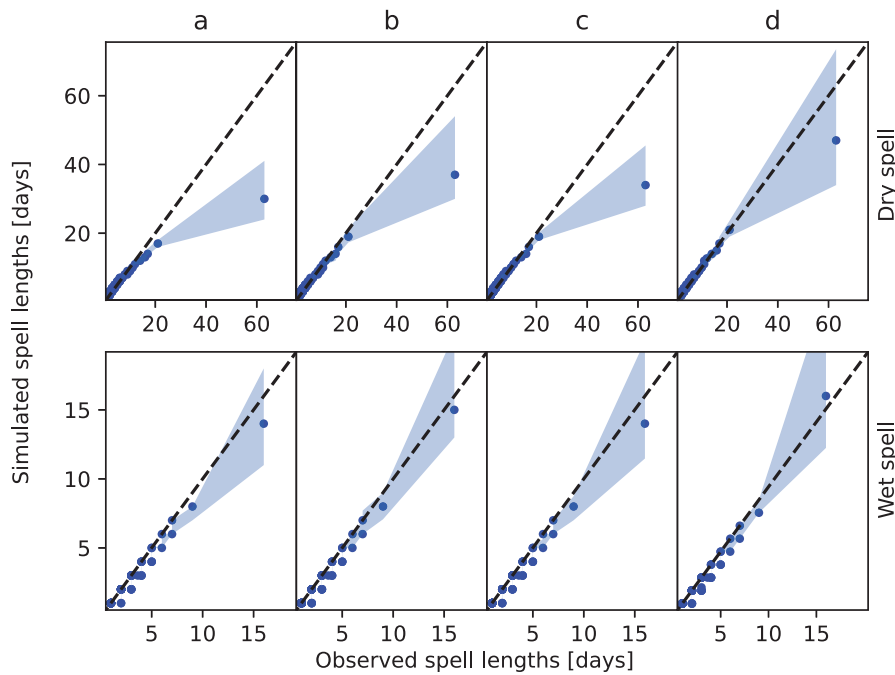


Fig. 5. QQ-plot of observed and simulated dry (top row) and wet (bottom row) spell lengths for the different Markov chains (a: first order, b: second order, c: first-order stochastically updated, d: second-order stochastically updated). The shaded area shows the total ensemble spread of 100 model realizations. The dashed line indicates the 1-to-1 line. The resolution of the QQ-plot is 1%.

4.2. Mean annual and seasonal precipitation

Since one of the main purposes of CON-SST-RAIN is to recreate continuous rainfall time series, the annual mean precipitation

should be represented sufficiently while still capturing seasonal rainfall variability. For each of the 100 CON-SST-RAIN realizations, the annual/seasonal averages are calculated over the length of the generated series and presented in Fig. 6 as boxplots, along with the annual/seasonal averages based on the six long-term rain gauges (in

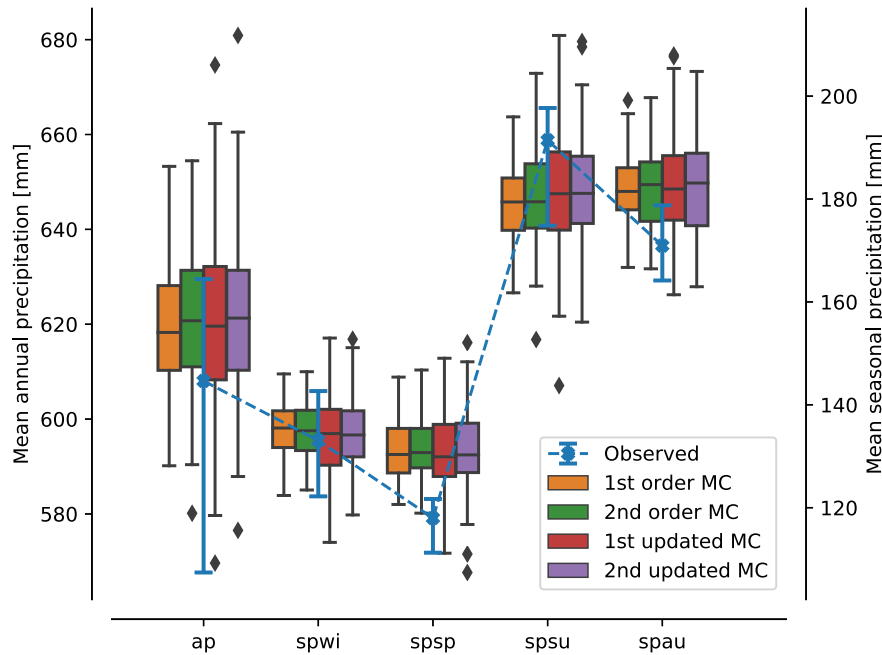


Fig. 6. Point scale mean annual precipitation (ap) and seasonal precipitation (winter: spwi, spring: spsp, summer: spsu, autumn: spau) for: observed stations (blue, long-term rain gauges from Fig. 1) and resampling realizations using the different types of Markov chains for sequential modelling for dry/wet days (orange: first order, green: second order, red: first order stochastically updated and purple: second order stochastically updated). Error bars indicate the 95% confidence band for 100 realizations for each of the Markov Chains. Error bars on the observed data depicts total range in rain gauge records with the cross indicating mean values across all included gauges. (For interpretation of the references to colour in this figure legend, the reader is referred to the web version of this article.)

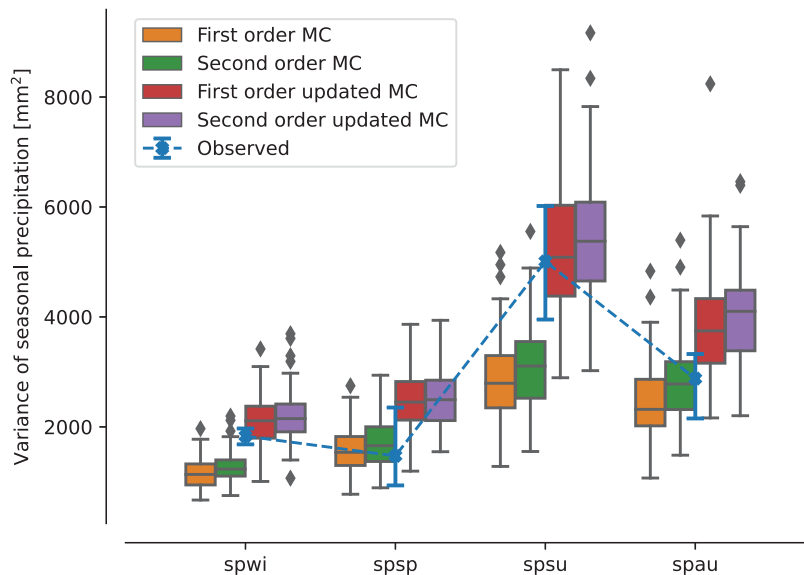


Fig. 7. Boxplots of inter-annual seasonal precipitation variance (spwi: winter, spsp: spring, spsu: summer, spau: autumn) for each of the investigated Markov Chain configurations. The boxplots are based on 100 realizations of CON-SST-RAIN for each Markov Chain configuration. The blue lines show the inter-annual seasonal precipitation variance ranges observed by the long-term rain gauge stations.

blue). The rain gauge averages are presented with minimum, mean, and maximum values since the dataset only represent six values for the annual and seasonal aggregations.

The Markov chain configurations perform similarly, with a tendency to overestimate the annual precipitation compared to the observed gauge data. Generally, the ensemble variabilities for the four configurations are within the station variability for the mean annual precipitation. Furthermore, CON-SST-RAIN is able to capture the overall seasonal variation, however, with an overestimation of spring and autumn precipitation and a underestimation of summer precipitation relative to

the observed gauge data. Scale differences between radar and gauge rainfall products most likely cause the underestimation of summer rainfall. Summer rainfall consists primarily of short-duration, high intensity, cloudbursts which in several studies (Thorndahl et al., 2019; Schleiss et al., 2020) has shown more significant variance between the two rainfall products, with radar data generally underestimating. This is also visible from the bias listed in Table 1. The overestimation of CON-SST-RAIN ensembles in the spring and autumn periods is less than 8% on average. The differences might be explained by the nature of low-intensity rainfall, which generally is poorly measured by the

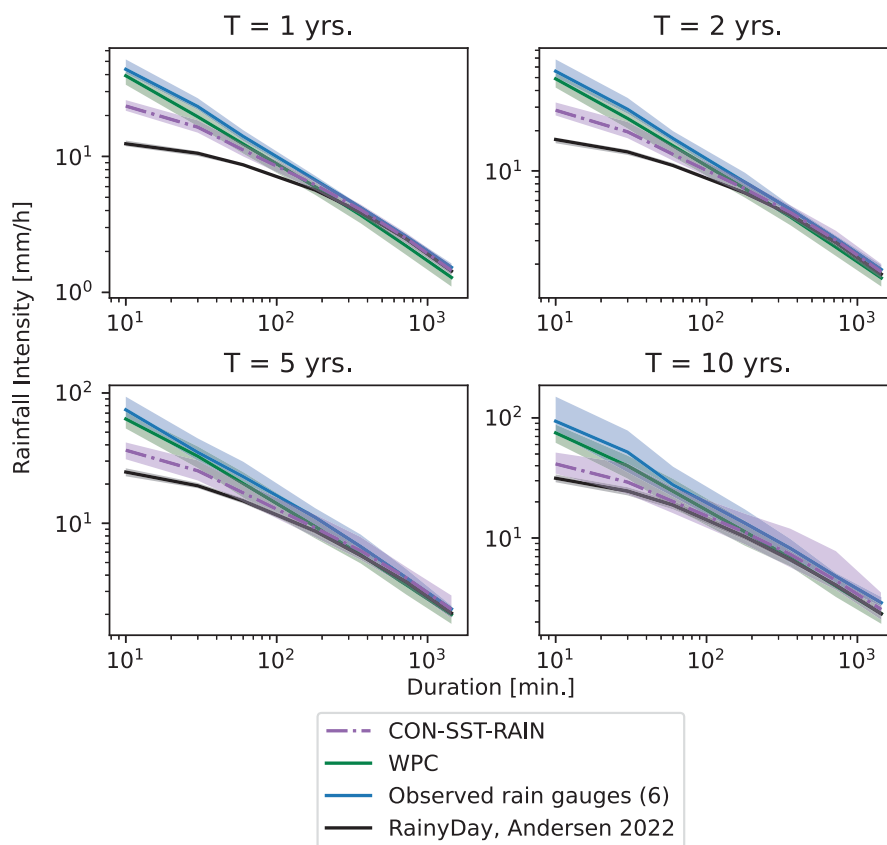


Fig. 8. IDF curves, for rainfall duration ranging from 10 min to 24 h, at point scale, derived from: CON-SST-RAIN (purple), WPC model (green), long term rain gauges (blue) and RainyDay (black). The shaded area indicates: ensemble range for CON-SST-RAIN and RainyDay, total range of the six rain gauges applied and 95% confidence intervals of the WPC model. (For interpretation of the references to colour in this figure legend, the reader is referred to the web version of this article.)

rain gauges. For the applied rain gauge network, a part of the data processing is discarding individual events consisting of only one tip (0.2 mm). The fraction of the total rainfall, which, for this reason, is discarded in the rain gauge records, is unknown, but it is suspected to be a significant portion of the annual precipitation which might explain why CON-SST-RAIN overestimates relative to the observed gauge data. On the other hand, the station variability in the seasonal averages also varies within approx. $\pm 5\%$. If more long-term gauges were available, a larger range of the seasonal averages would probably show, and the CON-SST-RAIN boxplots would overlap the rain gauge range values.

Generally, since differences in annual and seasonal averages are less than $\pm 10\%$, and due to the differences in spatial scales and data quantity between CON-SST-RAIN ensembles and rain gauge data, we do not consider this a hinder to continuing the evaluation of the proposed framework.

4.3. Low-frequency variability

In addition to average yearly and seasonal accumulations, CON-SST-RAIN's ability to simulate inter-annual variability of seasonal and monthly precipitation is essential for its applicability in hydrological assessment studies. The boxplots in Fig. 7 show the ensemble variance of the year-to-year seasonal precipitation for each Markov Chain configuration.

A large part of the variance in the CON-SST-RAIN ensemble can most likely be credited to the stochastic nature of the method (e.g. spatio-temporal sampling of rainfall events and variance in available rainfall data, Table 2). Adding an additional level of randomness should inevitably increase the variability. This is also evident in Fig. 7, when comparing the results of traditional Markov Chains to the stochastically

updated ones. The idea behind having a new Markov Chain for each simulated year is to increase the likelihood of having long chains of days with or without rain, increased likelihood of drought seasons, or periods of sustained rainfall. The stochastically updated Markov approach does indeed increase the variability of all seasons (median values on the box plot, Fig. 7) resulting in summer and winter variability to be similar to the observed gauge values. However, for spring and autumn, the updated Markov approach indicates a lower natural inter-annual variation; therefore, the mean variances of these seasons are slightly overestimated when comparing the observed data (blue cross, Fig. 7) to the CON-SST-RAIN ensemble. In this comparison it is also worth noticing that a higher variability is to be expected from a 100-member ensemble compared to an ensemble of six observational rain gauge series, and that some of the gauges however show comparable variation to that of the CON-SST-RAIN values. Therefore, we acknowledge that adding the updated Markov framework to CON-SST-RAIN increases the inter-annual variability of seasonal precipitation to a level similar to observed variation and choose the second-order stochastically updated Markov Chain as the preferred method of simulating day-to-day sequences of rain/no rain in the rest of the study.

4.4. Extreme value statistics

We generate 42 years of synthetic areal rainfall using CON-SST-RAIN with the second-order updated Markov chain scheme. We derive Intensity-Duration-Frequency (IDF) curves at point (Fig. 8) and areal scale (Fig. 9) using the partial duration series approach and California ranking as explained in Section 3.4. The IDF curves show extreme values statistics of rainfall at different rainfall durations (10 min to 24 h). We also include IDF curves obtained from the six long-term rain

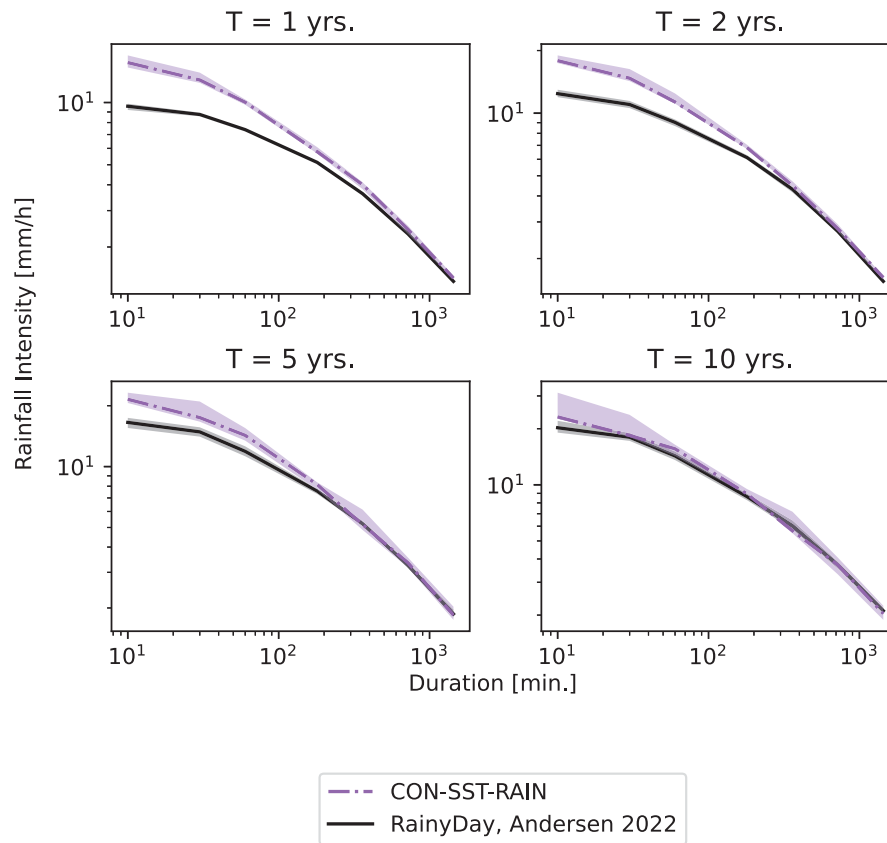


Fig. 9. IDF curves, for rainfall duration ranging from 10 min to 24 h, at catchment scale, derived from: CON-SST-RAIN (purple) and RainyDay, Andersen et al. (2022) (black). The shaded area indicates total ensemble range. (For interpretation of the references to colour in this figure legend, the reader is referred to the web version of this article.)

gauges each covering 42 years of recorded rainfall. IDF curves derived using the Danish regional extreme value model (WPC), as detailed in Gregersen et al. (2013) is included in the point-based analysis for comparison. IDF curves generated by the SST framework, through the RainyDay framework (Wright et al., 2017) with modifications as detailed in Andersen et al. (2022), are also included for both point and catchment scale.

At storm durations above three hours CON-SST-RAIN performs equally to the other shown methods with only a slight overestimation compared to the RainyDay and WPC IDF curves. However, the difference is negligible and within uncertainty levels. At sub-three-hour storm durations, CON-SST-RAIN and RainyDay SST IDF curves underestimate relative to the gauge-based IDF's. A similar phenomenon has been observed in Peleg et al. (2013, 2018) and Andersen et al. (2022). Specifically in Andersen et al. (2022), where extreme statistics are derived directly from the radar dataset (same as utilized in this study), using traditional approaches (Peak-Over-Threshold sampling and fitting to a Generalized-Pareto distribution), still shows underestimation compared to gauge based statistics. Scale differences are to be expected when comparing a radar pixel covering an area of 0.25 km² against a rain gauge that only covers a few square centimeters. This is also known as sub-pixel variability.

Fig. 9 compares area IDF's derived through CON-SST-RAIN and RainyDay. The IDF curves correspond to average area rainfall over the catchment of 150 km². Among the methods compared earlier, RainyDay and CON-SST-RAIN are the only methods that consider the spatial variability of rainfall, and therefore we do not compare to observed rain gauge data nor WPC IDF-curves considering area IDF's.

We note similar tendencies of significant discrepancies at short rainfall durations and similar agreements at longer durations. Although both sets of IDF curves are derived from the same base dataset, there

are still some discrepancies in data sampling and length of generated rain series. CON-SST-RAIN is generated from a sampling of whole days, whereas RainyDay (Andersen et al., 2022) has different storm catalogues for different durations. Furthermore, CON-SST-RAIN is generated for a total period of 42 years, whereas RainyDay is generated statistically as 1000-year series. For CON-SST-RAIN, this leads to a larger variability as function of return period (as seen at the 10-year return period in Fig. 9). As documented in Andersen et al. (2022) and Wright et al. (2017) RainyDay tends to underestimate intensities at short durations. Therefore, along with the conclusions of point scale IDF (Fig. 8), we consider CON-SST-RAIN to provide more realistically extreme areal statistics than RainyDay (Andersen et al., 2022).

4.5. Spatial correlation

Besides comparing extreme event statistics at point and aggregated catchment scales, it is also relevant to examine how well CON-SST-RAIN preserves the spatial variability of rainfall within the catchment. We do this by calculating the spatial correlation of daily rainfall accumulations as a function of distance and compare to the average spatial correlation from observed rain gauge data. Fig. 10 shows the spatial correlation (Pearson's r) for both observed data (all gauges shown in Fig. 1) and spatio-temporal rainfall generated by CON-SST-RAIN for days with more and less than 3 mm rain, respectively. The continuous data refers to correlations estimated, including points/pixels with zero-value data, and the groups marked by "simultaneous" include only positive data pairs.

For days with more than 3 mm rainfall CON-SST-RAIN shows comparable results to the observed gauge data with only a slightly higher daily spatial correlation as function of distance. The difference can be

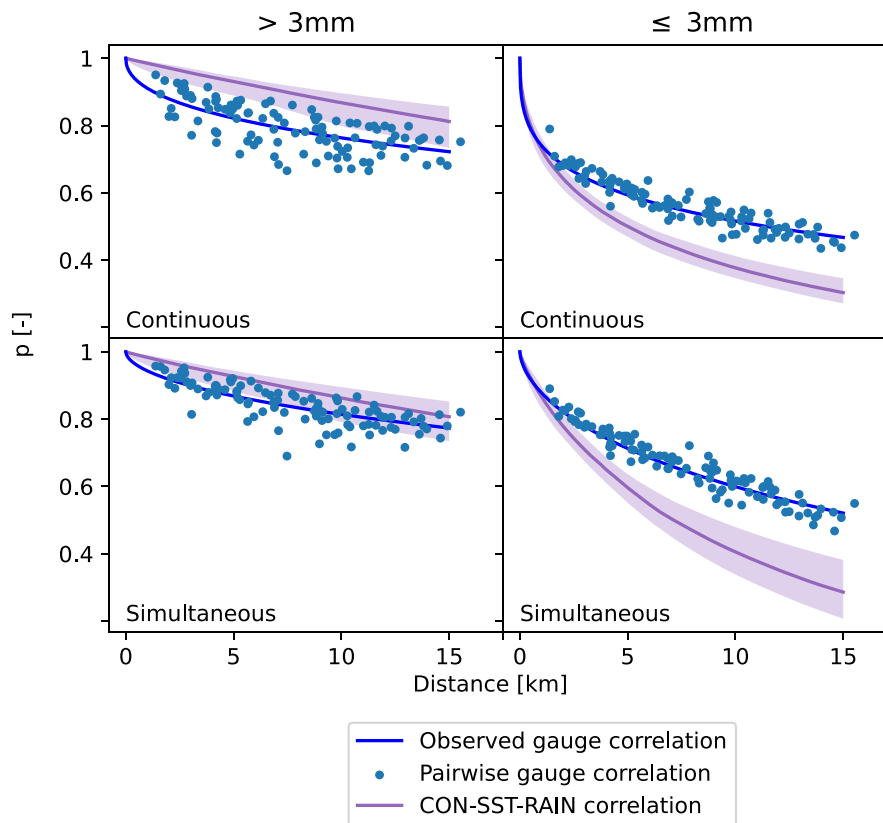


Fig. 10. Daily spatial correlation for observed rain gauge data (blue line) and CON-SST-RAIN (purple line, shaded area indicates 95% confidence interval of the 100 CON-SST-RAIN realizations). Blue dots indicates Pearson correlations (4) values for each gauge-pair that is fitted to Eq. (5). (For interpretation of the references to colour in this figure legend, the reader is referred to the web version of this article.)

sought in data quantity, but also the scale difference between point and radar pixel.

A more significant difference between observed and CON-SST-RAIN is noticed for the sub-3 mm values of spatial correlation, where CON-SST-RAIN in this case shows less spatial correlation than the rain gauge dataset. We speculate that the differences in data quantity or the sampling and processing of the radar data can cause this discrepancy. Proportionally the radar dataset contains fewer days with low rainfall intensities than the rain gauge dataset due to the implementation threshold criteria for valid bias adjustment. Furthermore, in the data processing, it can be difficult to distinguish between very low intensity and different kind of noise and clutter (that the overall filtering did not catch). By applying a drizzle threshold we try to eliminate as much of this noise as possible, but it appears that some is still present, by the underestimation of spatial correlation for low intensity rainfall. The rapid descending spatial correlation indicates a more random rainfall field which can be explained by common radar noise.

The difference between the continuous and simultaneous, above 3 mm values, is most likely a product of our assumption that the given Markov Chain is valid for the entire area. The stochastic transposition does not take into account that some of the precipitation sites might be dry. A naive approach of using day-to-day sequences of wet/dry states from all the short-term gauges as a replacement of stochastic sequence modelling with Markov Chain, instead of the entire CON-SST-RAIN framework, was tested (but not presented in this study). The days with rain are still simulated using the SST approach however, areas with zero rainfall, from the derived sequence, are forced to zero values. This approach does improve the spatial correlation however, without applying the generated rainfall to any kind of model the consequence of this approach can be difficult to determine.

5. Conclusion

This study presents a novel framework CON-SST-RAIN: a stochastic rainfall generator specialized for generating continuous space-time series for urban drainage design and planning. CON-SST-RAIN is based on Markov Chains for day-to-day sequences of dry/wet days, and substitutes stochastically transposed storms from spatiotemporal weather radar data on wet days. We present a method of stochastically updating Markov chains for passing years to incorporate low-frequency variation of inter-annual rainfall values better. CON-SST-RAIN is tested against multi-year records of rain gauges both at point and catchment scale. We show that, for the most part updating the Markov Chains by each passing year has negligible effects on mean annual/seasonal precipitation and dry/wet spell durations. However, updating the Markov chains by each passing year improves the inter-annual rainfall variation.

Extreme rain rates are well preserved in CON-SST-RAIN compared to observed gauge data and to the original SST framework (RainyDay, Andersen et al. (2022)) at both point and catchment scales. We observe a better representation of sub-hourly extremes when using CON-SST-RAIN compared to RainyDay. There are, however, still some underestimation of short-duration extreme intensities comparing CON-SST-RAIN and RainyDay outputs to rain gauge observations. This, is not necessarily an error in the proposed framework, but related to differences in scaling comparing point and pixel values as well as an artifact of daily mean field bias adjustment of radar data. An added benefit of CON-SST-RAIN over RainyDay is that all storm durations can be represented by daily values and do not need to be subdivided into duration-specific storm catalogs.

The spatial structure of the rainfall fields generated by CON-SST-RAIN closely resembles the spatial structure observed by rain gauges at a daily time scale. Low intensity rainfall is, however, less precisely

represented in comparison with rain gauge data. This shown difference might be caused by problems in the stochastic sampling of radar data or the assumption of a single Markov chain being valid for the entire area of interest. On the other hand, the differences might also be caused by the fact that we are comparing two different datasets with different quantities and scales and, therefore, should not expect to have completely aligned values comparing point gauge data with gridded radar data.

Overall, the suggested approach holds promising potential for producing stochastic rainfall inputs for hydrological models that require consideration of spatiotemporal rainfall variability to accurately simulate the hydrological response. The ability to generate ensembles can be used to investigate uncertainties in the hydrological response due to rainfall variability. Furthermore, in areas with no or short radar rainfall series available (or other high-resolution space–time rain input), CON-SST-RAIN can provide an alternative input to hydrological long-term simulation modelling. By adjusting target parameters, the stochastic framework can be applicable to climatological regions beyond the area from which the data is originally observed or adapted to be representative of future climate scenarios. The latter has been proposed by Thorndahl et al. (2017a), Sørup et al. (2017, 2018), Thorndahl and Andersen (2021) for point time series, but will most certainly also be a future development for spatiotemporal rainfall series as an extension of this study.

CRediT authorship contribution statement

Christoffer B. Andersen: Conceptualization, Formal analysis, Methodology, Software, Visualization, Writing – original draft, Investigation. **Daniel B. Wright:** Conceptualization, Resources, Software, Supervision, Writing – review & editing. **Søren Thorndahl:** Data curation, Formal analysis, Funding acquisition, Project administration, Supervision, Validation, Writing – review & editing.

Declaration of competing interest

The authors declare that they have no known competing financial interests or personal relationships that could have appeared to influence the work reported in this paper.

Data availability

The authors do not have permission to share data.

Acknowledgements

The authors would like to acknowledge and thank the Danish Meteorological Institute (DMI) for providing and processing the radar data applied in this study. Likewise we would like to thank the Danish Water Pollution Committee (WPC) within IDA: The Danish Society of Engineers for the use of rain gauge data. This study received partial funding from the Foundation for Development of Technology in the Danish Water Sector, Project: CLIMACS, Grant/Award Number: 1162.2017, as well as from Aarhus Water Utility in Denmark.

References

Andersen, C.B., Wright, D.B., Thorndahl, S., 2022. Sub-hourly to daily rainfall intensity-duration-frequency estimation using stochastic storm transposition and discontinuous radar data. *Water* 14 (24), <https://dx.doi.org/10.3390/w14244013>.
 Brissette, F., Khalili, M., Leconte, R., 2007. Efficient stochastic generation of multi-site synthetic precipitation data. *J. Hydrol.* 345 (3–4), 121–133. <https://dx.doi.org/10.1016/j.jhydrol.2007.06.035>.
 Burton, A., Kilsby, C., Fowler, H., Cowpertwait, P., O'Connell, P., 2008. RainSim: A spatial-temporal stochastic rainfall modelling system. *Environ. Model. Softw.* 23 (12), 1356–1369. <https://dx.doi.org/10.1016/j.envsoft.2008.04.003>.

Cristiano, E., ten Veldhuis, M.C., van de Giesen, N., 2017. Spatial and temporal variability of rainfall and their effects on hydrological response in urban areas – a review. *Hydrol. Earth Syst. Sci.* 21 (7), 3859–3878. <https://dx.doi.org/10.5194/hess-21-3859-2017>.
 Cristiano, E., ten Veldhuis, M.-c., Wright, D.B., Smith, J.A., van de Giesen, N., 2019. The influence of rainfall and catchment critical scales on urban hydrological response sensitivity. *Water Resour. Res.* 55 (4), 3375–3390. <https://dx.doi.org/10.1029/2018WR024143>.
 Einfalt, T., Arnbjerg-Nielsen, K., Golz, C., Jensen, N.-E., Quirnbach, M., Vaes, G., Vieux, B., 2004. Towards a roadmap for use of radar rainfall data in urban drainage. *J. Hydrol.* 299 (3), 186–202. <https://dx.doi.org/10.1016/j.jhydrol.2004.08.004>.
 Fowler, H., Kilsby, C., O'Connell, P., Burton, A., 2005. A weather-type conditioned multi-site stochastic rainfall model for the generation of scenarios of climatic variability and change. *J. Hydrol.* 308 (1–4), 50–66. <https://dx.doi.org/10.1016/j.jhydrol.2004.10.021>.
 Gregersen, I.B., Madsen, H., Rosbjerg, D., Arnbjerg-Nielsen, K., 2013. A spatial and nonstationary model for the frequency of extreme rainfall events. *Water Resour. Res.* 49 (1), 127–136. <https://dx.doi.org/10.1029/2012WR012570>, URL <https://agupubs.onlinelibrary.wiley.com/doi/abs/10.1029/2012WR012570>, arXiv:<https://agupubs.onlinelibrary.wiley.com/doi/pdf/10.1029/2012WR012570>.
 Gringorten, I.I., 1963. A plotting rule for extreme probability paper. *J. Geophys. Res.* 68 (3), 813–814. <https://dx.doi.org/10.1029/JZ068i003p00813>.
 Madsen, H., Gregersen, I.B., Rosbjerg, D., Arnbjerg-Nielsen, K., 2017. Regional frequency analysis of short duration rainfall extremes using gridded daily rainfall data as co-variate. *Water Sci. Technol.* 75 (8), 1971–1981. <https://dx.doi.org/10.2166/wst.2017.089>.
 Müller-Thomy, H., Wallner, M., Förster, K., 2018. Rainfall disaggregation for hydrological modeling: is there a need for spatial consistence? *Hydrol. Earth Syst. Sci.* 22 (10), 5259–5280. <https://dx.doi.org/10.5194/hess-22-5259-2018>.
 Nielsen, K.T., Moldrup, P., Thorndahl, S., Nielsen, J.E., Uggerby, M., Rasmussen, M.R., 2019. Field-scale monitoring of Urban Green Area rainfall-runoff processes. *J. Hydrol. Eng.* 24 (8), [https://dx.doi.org/10.1061/\(ASCE\)HE.1943-5584.0001795](https://dx.doi.org/10.1061/(ASCE)HE.1943-5584.0001795).
 Nielsen, J.E., Thorndahl, S., Rasmussen, M.R., 2014. A numerical method to generate high temporal resolution precipitation time series by combining weather radar measurements with a nowcast model. *Atmos. Res.* 138, 1–12. <https://dx.doi.org/10.1016/j.atmosres.2013.10.015>.
 Nielsen, J., van de Beek, C., Thorndahl, S., Olsson, J., Andersen, C., Andersson, J., Rasmussen, M., Nielsen, J., 2024. Merging weather radar data and opportunistic rainfall sensor data to enhance rainfall estimates. *Atmos. Res.* 300, 107228. <https://dx.doi.org/10.1016/j.atmosres.2024.107228>.
 Ochoa-Rodriguez, S., Wang, L.P., Gires, A., Pina, R.D., Reinoso-Rondinel, R., Bruni, G., Ichiba, A., Gaitan, S., Cristiano, E., van Assel, J., Kroll, S., Murlà-Tuyts, D., Tisserand, B., Schertzer, D., Tchiguirinskaia, I., Onof, C., Willems, P., ten Veldhuis, M.C., 2015. Impact of spatial and temporal resolution of rainfall inputs on urban hydrodynamic modelling outputs: A multi-catchment investigation. *J. Hydrol.* 531, 389–407. <https://dx.doi.org/10.1016/j.jhydrol.2015.05.035>.
 Peleg, N., Ben-Asher, M., Morin, E., 2013. Radar subpixel-scale rainfall variability and uncertainty: lessons learned from observations of a dense rain-gauge network. *Hydrol. Earth Syst. Sci.* 17 (6), 2195–2208. <https://dx.doi.org/10.5194/hess-17-2195-2013>.
 Peleg, N., Fatichi, S., Athanasios, P., Molnar, P., Burlando, P., 2017. An advanced stochastic weather generator for simulating 2-D high-resolution climate variables. *J. Adv. Model. Earth Syst.* 9 (3), 1595–1627. <https://dx.doi.org/10.3929/ethz-b-000190507>.
 Peleg, N., Marra, F., Fatichi, S., Paschalis, A., Molnar, P., Burlando, P., 2018. Spatial variability of extreme rainfall at radar subpixel scale. *J. Hydrol.* 556, 922–933. <https://dx.doi.org/10.1016/j.jhydrol.2016.05.033>.
 Peleg, N., Molnar, P., Burlando, P., Fatichi, S., 2019. Exploring stochastic climate uncertainty in space and time using a gridded hourly weather generator. *J. Hydrol.* 571, 627–641. <https://dx.doi.org/10.1016/j.jhydrol.2019.02.010>.
 Rajagopalan, B., Lall, U., 1999. A k-nearest-neighbor simulator for daily precipitation and other weather variables. *Water Resour. Res.* 35 (10), 3089–3101.
 Schleiss, M., Olsson, J., Berg, P., Niemi, T., Kokkonen, T., Thorndahl, S., Nielsen, R., Ellerbæk Nielsen, J., Bozhinova, D., Pulkkinen, S., 2020. The accuracy of weather radar in heavy rain: a comparative study for Denmark, the Netherlands, Finland and Sweden. *Hydrol. Earth Syst. Sci.* 24 (6), 3157–3188. <https://dx.doi.org/10.5194/hess-24-3157-2020>.
 Sharma, A., Mehrotra, R., 2010. Rainfall generation. In: Washington DC American Geophysical Union Geophysical Monograph Series, vol. 191, pp. 215–246. <https://dx.doi.org/10.1029/2010GM000973>.
 Smith, J.A., Krajewski, W.F., 1991. Estimation of the mean field bias of radar rainfall estimates. *J. Appl. Meteorol. Climatol.* 30 (4), 397–412. [https://dx.doi.org/10.1175/1520-0450\(1991\)030<0397:EOTMFB>2.0.CO;2](https://dx.doi.org/10.1175/1520-0450(1991)030<0397:EOTMFB>2.0.CO;2).
 Sørup, H.J.D., Davidsen, S., Löwe, R., Thorndahl, S.L., Borup, M., Arnbjerg-Nielsen, K., 2018. Evaluating catchment response to artificial rainfall from four weather generators for present and future climate. *Water Sci. Technol.* 77 (11), 2578–2588. <https://dx.doi.org/10.2166/wst.2018.217>.

- Sørup, H.J.D., Georgiadis, S., Bülow Gregersen, I., Arnbjerg-Nielsen, K., 2017. Formulating and testing a method for perturbing precipitation time series to reflect anticipated climatic changes. *Hydrol. Earth Syst. Sci.* 21 (1), 345–355. <http://dx.doi.org/10.5194/hess-21-345-2017>.
- Thejll, P., Boberg, F., Schmith, T., Christiansen, B., Christensen, O.B., Madsen, M.S., Su, J., Andree, E., Olsen, S., Langen, P.L., Madsen, K.S., Olesen, M., Pedersen, R.A., Payne, M.R., 2022. Methods used in the danish climate atlas. ISBN: 978-87-7478-690-0.
- Thomassen, E.D., Thorndahl, S.L., Andersen, C.B., Gregersen, I.B., Arnbjerg-Nielsen, K., Sørup, H.J.D., 2022. Comparing spatial metrics of extreme precipitation between data from rain gauges, weather radar and high-resolution climate model re-analyses. *J. Hydrol.* 610, 127915. <http://dx.doi.org/10.1016/j.jhydrol.2022.127915>.
- Thorndahl, S., 2009. Stochastic long term modelling of a drainage system with estimation of return period uncertainty. *Water Sci. Technol.* 59 (12), 2331–2339. <http://dx.doi.org/10.2166/wst.2009.305>.
- Thorndahl, S., Andersen, C.B., 2021. CLIMACS: A method for stochastic generation of continuous climate projected point rainfall for urban drainage design. *J. Hydrol.* 602, 126776. <http://dx.doi.org/10.1016/j.jhydrol.2021.126776>.
- Thorndahl, S., Andersen, A.K., Larsen, A.B., 2017a. Event-based stochastic point rainfall resampling for statistical replication and climate projection of historical rainfall series. *Hydrol. Earth Syst. Sci.* 21 (9), 4433–4448. <http://dx.doi.org/10.5194/hess-21-4433-2017>, URL <https://hess.copernicus.org/articles/21/4433/2017/>.
- Thorndahl, S., Einfalt, T., Willems, P., Nielsen, J.E., ten Veldhuis, M.C., Arnbjerg-Nielsen, K., Rasmussen, M.R., Molnar, P., 2017b. Weather radar rainfall data in urban hydrology. *Hydrol. Earth Syst. Sci.* 21 (3), 1359–1380. <http://dx.doi.org/10.5194/hess-21-1359-2017>.
- Thorndahl, S., Nielsen, J.E., Rasmussen, M.R., 2014a. Bias adjustment and advection interpolation of long-term high resolution radar rainfall series. *J. Hydrol.* 508, 214–226. <http://dx.doi.org/10.1016/j.jhydrol.2013.10.056>.
- Thorndahl, S., Nielsen, J.E., Rasmussen, M.R., 2019. Estimation of storm-centred areal reduction factors from radar rainfall for design in urban hydrology. *Water* 11 (6), 1013. <http://dx.doi.org/10.3390/w11061013>.
- Thorndahl, S., Smith, J.A., Baeck, M.L., Krajewski, W.F., 2014b. Analyses of the temporal and spatial structures of heavy rainfall from a catalog of high-resolution radar rainfall fields. *Atmos. Res.* 144, 111–125. <http://dx.doi.org/10.1016/j.atmosres.2014.03.013>.
- Tuyls, D.M., Thorndahl, S., Rasmussen, M.R., 2018. Return period assessment of urban pluvial floods through modelling of rainfall–flood response. *J. Hydroinformatics* 20 (4), 829–845. <http://dx.doi.org/10.2166/hydro.2018.133>.
- Villarini, G., Krajewski, W.F., 2010. Review of the different sources of uncertainty in single polarization radar-based estimates of rainfall. *Surv. Geophys.* 31 (1), 107–129. <http://dx.doi.org/10.1007/s10712-009-9079-x>.
- Wilks, D.S., Wilby, R.L., 1999. The weather generation game: a review of stochastic weather models. *Prog. Phys. Geogr.* 23 (3), 329–357.
- WPC, 2007. Funktionspraksis for afløbssystemer under regn, skrift nr. 27 (Practice for drainage systems during rain, Guideline no. 27) The Water Pollution Committee (WPC) of the Society of Danish Engineers.
- Wright, D.B., Mantilla, R., Peters-Lidard, C.D., 2017. A remote sensing-based tool for assessing rainfall-driven hazards. *Environ. Model. Softw.* 90, 34–54. <http://dx.doi.org/10.1016/j.envsoft.2016.12.006>.
- Wright, D.B., Smith, J.A., Baeck, M.L., 2014. Flood frequency analysis using radar rainfall fields and stochastic storm transposition. *Water Resour. Res.* 50 (2), 1592–1615. <http://dx.doi.org/10.1002/2013wr014224>.
- Wright, D.B., Smith, J.A., Villarini, G., Baeck, M.L., 2013. Estimating the frequency of extreme rainfall using weather radar and stochastic storm transposition. *J. Hydrol.* 488, 150–165. <http://dx.doi.org/10.1016/j.jhydrol.2013.03.003>.
- Wright, D.B., Yu, G., England, J.F., 2020. Six decades of rainfall and flood frequency analysis using stochastic storm transposition: Review, progress, and prospects. *J. Hydrol.* 585, 124816. <http://dx.doi.org/10.1016/j.jhydrol.2020.124816>.
- Zhou, L., Meng, Y., Abbaspour, K.C., 2019. A new framework for multi-site stochastic rainfall generator based on empirical orthogonal function analysis and Hilbert-huang transform. *J. Hydrol.* 575, 730–742. <http://dx.doi.org/10.1016/j.jhydrol.2019.05.047>.
- Zhou, Z., Smith, J.A., Baeck, M.L., Wright, D.B., Smith, B.K., Liu, S., 2021. The impact of the spatiotemporal structure of rainfall on flood frequency over a small urban watershed: An approach coupling stochastic storm transposition and hydrologic modeling. *Hydrol. Earth Syst. Sci.* 25 (9), 4701–4717. <https://doi.org/10.5194/hess-25-4701-2021>.